ELSEVIER

Journal of Photochemistry and Photobiology A: Chemistry 130 (2000) 35–47

Journal of Photochemistry and Photobiology A:Chemistry

www.elsevier.nl/locate/jphotochem

Photodegradation of the aminoazobenzene acid orange 52 by three advanced oxidation processes: UV/H_2O_2, UV/TiO_2 and VIS/TiO_2 Comparative mechanistic and kinetic investigations

Catherine Galindo [a,*], Patrice Jacques [b], André Kalt [a]

[a] *Laboratoire de Chimie Textile, Ecole Nationale Supérieure de Chimie de Mulhouse, 3 rue A. Werner, F 68093 Mulhouse, France*

[b] *Département de Photochimie Générale, UMR CNRSN° 7525, Ecole Nationale Supérieure de Chimie de Mulhouse, 3 rue A. Werner, F 68093 Mulhouse, France*

Received 19 July 1999; accepted 24 September 1999

Abstract

This paper presents the results obtained from the oxidation of the aminoazobenzene dye AO52 by the UV/H_2O_2, UV/TiO_2 and VIS/TiO_2 systems. In the former case, we investigated the formation of first by-products by means of GC/MS, HPLC and ^{1}H NMR. spectroscopy. We conclude that hydroxyl radicals are added to aromatic rings in the ipso position with respect to the sulfonate group or to the azo-linkage-bearing carbon. The reaction of the inorganic radical with the *N,N*-dimethylamino substituent, leading to demethylation, adds to the multiplicity of the possible pathways. Degradation by the UV/TiO_2 system is pH dependent. Whereas hydroxyl radicals are the main oxidative agent in neutral and alkaline solutions, positive hole-induced oxidation competes with the reduction of the protonated dye molecules in acid media. Moreover, FTIR spectroscopy of AO52/TiO_2 wafers provided an insight to the nature of the photoproducts. This process is very efficient since only ultimate breakdown products, i.e. aliphatic acids and inorganic salts, are detected. Similar results were obtained using visible light as the irradiation source in the case of wafers whereas in heterogeneous solutions, the dye seems to be resistant to degradation.

Keywords: Azo dye; Advanced oxidation processes; Kinetics; Degradation products

1. Introduction

Due to an increasing environmental pollution and the establishment of stringent standards for rejecting wastewaters, purification of industrial aqueous effluents is getting more and more importance. Now, advanced oxidation processes (AOPs), where highly oxidizing species, like hydroxyl radicals, are produced, can provide a convenient way of treating undesirable chemicals, for instance pesticides, halogenated benzenes and dyes [1–4]. They are notably known to discolour several structurally different sulfonated hydroxyazo dyes [5–7]. However, only few informations are available about the reactivity of aminoazodyes and about the nature of their degradation products. Further, intermediates should not be neglected, because they can take part in the degradation process either by reacting with the oxidant or by absorbing photons. Moreover, they may be more toxic than the original compound.

In the first part of the present report, the main products of the reaction of hydroxyl radicals, generated upon photolysis of hydrogen peroxide, with an aminoazobenzene dye, AO52 are identified. The reaction sites on the organic molecule and the possible mechanisms involved are discussed. It is worth noting that the main drawbacks of the above-mentioned photochemical methods are the necessity to use rigid ultraviolet and the low extinction coefficient of hydrogen peroxide. To lessen the impact of these problems, heterogeneous systems with titanium dioxide as a photocatalyst may be used for water purification. Our objectives were to determine how the photocatalytic (UV/TiO_2) and photosensitizing (VIS/TiO_2) degradation pathways differ from that corresponding to the action of UV radiations in the presence of hydrogen peroxide. These comparisons are expected to provide some insight into the basic mechanisms of the TiO_2-assisted water treatment.

* Corresponding author.

E-mail addresses: c.galindo@univ-mulhouse.fr (C. Galindo), p.jacques@univ-mulhouse.fr (P. Jacques)

1010-6030/00/$ – see front matter
PII: S1010-6030(99)00199-9

2. Experimental details

2.1. Reagents

Hydrogen peroxide (30%, w/w), HPLC grade solvents (water and methanol), pyridine, diethylether, sodium hydrogenocarbonate, sodium sulfate, sodium acetate, copper sulfate and chromium sulfate were purchased from Prolabo. Diethylether was distilled before use. Distilled water was used throughout. The surfactants Albegal SET and Albegal FFA were from Ciba Geigy. Titanium dioxide particules were supplied by Degussa (P25). This material is mainly anatase. It has a BET surface area of approximately $50\,m^2\,g^{-1}$ and a mean particule size of 30 nm. The dyes AO52, A07, AR2 and AO5 are respectively Aldrich and Fluka products. They were used without further purification.

2.2. Photoreactors and light sources

For the UV/H_2O_2 and UV/TiO_2 processes, irradiations were performed in a batch photoreactor of 1 l in volume with, respectively, a 15 W low-pressure mercury lamp (Philips, emission: 253.7 nm) or a 18 W black-light mercury lamp (Philips, $\lambda > 310$ nm). For the VIS/TiO_2 system, an He–Cd laser (Kimmon), generating a 442 nm monochromatic light, was positioned in front of a 3 ml pyrex vessel.

2.3. Procedures

The desired concentration of the dye and the loading of TiO_2 or H_2O_2 were fed in the reactor. The aqueous solutions were magnetically stirred. The pH of the solution was adjusted using dilute nitric acid or aqueous sodium hydroxide solutions. After 30 mm of premixing, the lamp was started to initiate the reaction. At regular time intervals, samples were taken and, when appropriate, filtrated on a 0.45 μm syringe filter. The remaining dye content was determinated using a Kontron Uvikon 943 spectrophotometer. UV–VIS spectra were recorded between 190 and 650 nm. The total organic carbon (TOC) value was obtained using a IONICS carbon analyzer and the electric conductivity using a WTW conductimeter. The sulfur mineralization rate was determinated by nephelometry, after adding some barium chloride to the solution.

The adsorption isotherms were obtained by prolonged agitation of the catalyst in dye solutions of varying concentrations, followed by a spectrophotometric estimation of the dye remaining in the solution. All isotherm measurements were made in the dark.

2.4. FTIR analysis

AO52 (1.2×10^{-4}–2.4×10^{-4} M) was adsorbed on titanium dioxide particules ($5\,g\,l^{-1}$). The residue was dried at 70°C. A wafer was made by pressing about 30 mg of powder in a laboratory press at 7.5 bars. It was then irradiated using either the He–Cd laser or the blacklight lamp. FTIR spectra were periodically recorded using a Nicolet 710 spectrometer. Absorbance spectra were measured in the 1000–1900 cm^{-1} region with a resolution of $4\,cm^{-1}$. Titanium dioxide was used as a background reference.

2.5. Detection of break down products

Sodium hydroxide was added to the irradiated solution (pH >13) and extracted five times with diethyether. The combined extracts were dried over sodium sulfate and evaporated. The residue was then analysed by GC/MS or HPLC. The remaining aqueous solution was evaporated under reduced pressure, esterified using first thionyl chloride, then methanol/pyridine and finally analysed by GC/MS. Analysis were performed on an analytical mass spectrometer fitted with a Hewlett–Packard 5890 Series II GC apparatus containing a capillary column (25 m long, 0.15 mm in width). A temperature gradient was used in the separation. The temperature was maintained at 80°C for 3 min and then increased to 310°C at a rate of 3.4°C/min. HPLC analyses were realized on a Waters 600E apparatus, using a C-18 reversed phase column (Nucleosil 15 cm × 4.6 mm) and a gradient eluent consisting of water and methanol. The methanol concentration was maintained at 20% for 5 min, then increased to 100% in 15 min, and finally maintained at 100% for 5 min. Compound elution was monitored at 210 nm.

2.6. ^1H NMR spectra

^1H NMR spectra were recorded on a Brucker AC 250.13 MHz spectrometer.

Compound 9: 3.08 ppm (s, 6H) −5.40 ppm (s, 1H) −6.75 ppm (d, 2H, $J = 9.1$ Hz) 6.91 ppm (d, 2H, $J = 8.8$ Hz) −7.79 ppm (d, 2H, $J = 8.8$ Hz) −7.83 ppm (d, 2H, $J = 9.1$ Hz).

Compound 10 : 2.92 ppm (s, 3H) −5.55 ppm (s, 1H) −6.65 ppm (d, 2H, $J = 8.9$ Hz) 6.91 ppm (d, 2H, $J = 8.9$ Hz) −7.78 ppm (d, 2H, $J = 8.9$ Hz) −7.80 ppm (d, 2H, $J = 8.9$ Hz).

3. Results and discussion

AO52 was chosen as a model for hydrosoluble aminoazobenzenes, due to the toxicity associated with this class of compounds and to its chemical resistance to degradation.

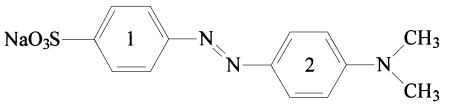

Fig. 1 presents its absorption spectrum in water at pH 5.9, for which no protonation of the azo bond and of the sulfonate group can occur. The powerful electron-donating dimethylamino group generates a $\pi \rightarrow \pi^*$ transition which

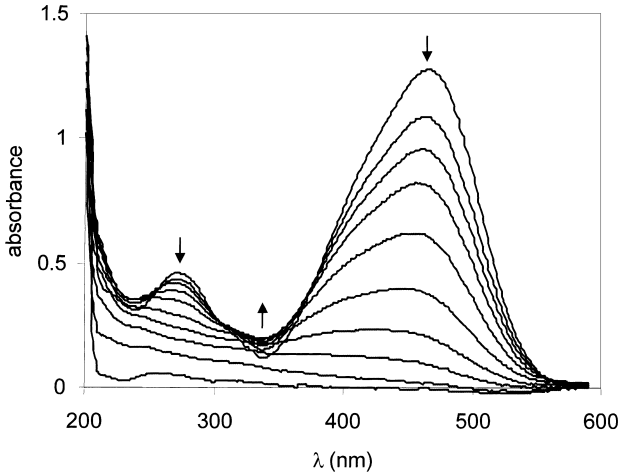

Fig. 1. Evolution of the UV–VIS spectrum under UV irradiation of an aqueous solution containing AO52 (10^{-3} M) and hydrogen peroxide (2×10^{-1} M). Solutions were diluted before recording.

lies in the visible region of the spectrum ($\lambda_{max} = 463$ nm). The molar extinction coefficient of this charge transfer transition is very high ($\varepsilon_{463} = 26.7 \times 10\,M^{-1}\,cm^{-1}$) because of the relatively large redistribution of electron density that occurs on excitation. The $\pi \rightarrow \pi^*$ transition located in the aromatic rings is responsible of the band at 270 nm.

3.1. Oxidation of the dye AO52 by the UV/H_2O_2 advanced oxidation process

3.1.1. Kinetic investigations

No discolouration occurs in an aqueous solution of AO52 and hydrogen peroxide in the dark, and the disappearance of the dye molecules was negligible by direct UV ($\lambda = 253.7$ nm) excitation, in the absence of an oxidant. But the combined action of UV and H_2O_2 induces a large decrease of the absorbance especially in the visible part of the spectrum, as illustrated in Fig. 1. Therefore, the drop of the absorbance results exclusively from the reaction between dye molecules and hydroxyl radicals, generated upon photolysis of H_2O_2. Moreover, the dosage in hydrogen peroxide is sufficient to maintain the concentration in hydroxyl radicals constant during the experiment and therefore for discussion of the reaction in terms of pseudo-first-order kinetics:

$$-\frac{dC}{dt} = kC \tag{1}$$

with C the concentration of the dye at time t; k the pseudo-first-order reaction rate constant

However, additional experiments showed that k depends on the concentration in hydrogen peroxide. Indeed, the low absorption coefficient of H_2O_2 in the accessible wavelength region requires rather high H_2O_2 concentrations. Now, $HO^\bullet$ radical efficiently reacts with hydrogen peroxide (Eq. (3)), so that the photo-decomposition promoter itself contributes to the $HO^\bullet$-scavenging capacity and reduces the efficiency of pollutant degradation, as illustrated in Fig. 2. For this reason, irradiation conditions must be carefully optimized to make the process cost-effective.

$$H_2O_2 + h\nu \rightarrow 2HO^\bullet \tag{2}$$

$$H_2O_2 + HO^\bullet \rightarrow HO_2^\bullet + H_2O \quad k = 2.7 \times 10^7\,M^{-1}\,s^{-1}\ [8] \tag{3}$$

On the other hand, we must consider that dyebath effluents generally contain a complex mixture of dyes, dispersing, leveling and wetting agents and traces of metals, especially copper and chromium salts. Additives are likely to modify the oxidation rate of the dye, either by competing for the oxidizing radicals or by absorbing light.

The simultaneous effect of surfactants and common anions (HCO_3^-, $CH_3CO_2^-$, SO_4^{2-}) at concentrations frequently present in industrial wastewaters was investigated by simulating textile effluents and the results are collected in Table 1. It is important to note that the reaction rate is lower than that obtained in deionized water, but longer irradiation times still lead to a complete discolouration of the solution. In fact, the failure of sulfate ions to decrease the oxidation rates adds support to the view that they are inefficient hydroxyl radical scavengers [9]. Moreover, their potential reaction with hydroxyl radical leads to the anion-radical $SO_4^{\bullet-}$, which may interact with organic matter. These reactions are generally diffusion-controlled [10]. Table 1 shows that, on the contrary, addition of bicarbonates or acetates to the solution yields an inhibition of the degradation. The radical-ion formed in reactions 4 and 5 show a much lower reactivity than the $HO^\bullet$ radical. They react only with compounds that can be readily oxidized.

$$HCO_3^- + HO^\bullet \rightarrow CO_3^{\bullet-} + H_2O \quad k_1 = 1.5 \times 10^7\,l\,mol^{-1}\,s^{-1}\ [11] \tag{4}$$

$$H_3C{-}CO_2^- + HO^\bullet \rightarrow H_2C^\bullet{-}CO_2^- + H_2O \quad k_2 = 4.3 \times 10^7\,l\,mol^{-1}\,s^{-1}\ [11] \tag{5}$$

Amphoteric surfactants such as Albegal SET and Albegal FFA, actually used in dyeing processes involving acid dyes, both consume sizable quantities of hydroxyl radicals and behave as inner filters, since they absorb light at 253.7 nm. Hence, the solution becomes more impermeable to UV radiations and the rate of photolysis of hydrogen peroxide, which directly depends on the fraction of radiation absorbed by H_2O_2, is sharply reduced.

Then, the influence of dissolved transition metal impurity ions on the photodegradation of AO52 was considered. Adding copper or chromium cations does not induce a change in the UV–VIS spectrum of the dye, but complexation of organic molecules by nitrogen atoms of the azo linkage cannot be excluded.

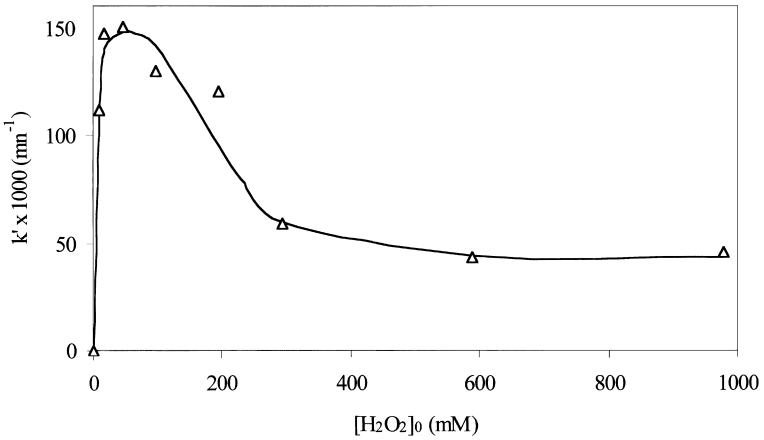

Fig. 2. Effect of the initial concentration of hydrogen peroxide on the oxidation rate of the dye AO52. $[AO52]_0 = 5.7 \times 10^{-5}$ M; initial pH = 5.9 – rT.

Table 2 shows that Cu^{2+} is much more efficient than Cr^{3+} in photo-Fenton-like systems. In the dark, Cu^{2+} is not able to induce the dye degradation, but it can initiate H_2O_2 decomposition, since, in the latter case, a slight decrease of the absorbance in the visible part is observed. Under light, the monovalent copper ion is produced (Eq. (6)), which efficiently reacts with hydrogen peroxide, leading to additional hydroxyl radicals (Eq. (7)) or regenerates Cu^{2+} (Eq. (8)). Cu^{2+} would also react with intermediary organic radicals, according to Eq. (9) and (10):

$$Cu^{2+} + HO_2^{\bullet} \rightarrow Cu^{+} + H^{+} + O_2 \quad (6)$$

$$Cu^{+} + H_2O_2 \rightarrow Cu^{2+} + HO^{\bullet} + HO^{-} \quad (7)$$

$$Cu^{+} + HO_2^{\bullet} \rightarrow Cu^{2+} + HO_2^{-} \quad (8)$$

$$RH + HO^{\bullet} \rightarrow R^{\bullet} + H_2O \quad (9)$$

$$R^{\bullet} + Cu^{2+} \rightarrow R^{+} + Cu^{+} \quad (10)$$

3.1.2. Degradation mechanism

The dye degradation is most effective in acid solution, as established from our earlier study where reaction rates at various pH were compared [12]. This behaviour is due to the high sensitivity to oxidation of the protonated form of the dye. In the present study, the reactivity of unprotonated dye molecules was just investigated. Note that, in the present case, a much more concentrated solution of the dye is used (10^{-3} M). However, the UV–VIS spectra recorded at various irradiation times are similar to those obtained with dilute solutions. Moreover, on the mechanistic viewpoint, analysis of these spectra is very instructive. Indeed, during the oxidative process, no clear isosbestic point can be detected. This suggests that there is no direct conversion of AO52 into a specific product and finally that degradation occurs through a number of stages. The chemical degradation of dye molecules with the concommittant production of lower-molecular-weight ionic by-products is also indicated by a raise of the conductivity of the solution from 105 to 610 $\mu S\,cm^{-1}$ in 275 min.

Table 1
Influence of the composition of the solution on the discolouration rate

Additive	[additive] (M)	k/kref
none	0	1
Hydrogenocarbonates	1.6×10^{-3}	0.80
Acetates	1.2×10^{-2}	0.66
Sulfates	2.0×10^{-2}	1
Albegal FFA + Albegal SET	0.5% w/w and 1.5% w/w	0.62
Simulated dye bath	above-mentioned additives	0.54

Table 2
Comparative study of the efficiency of the UV/H_2O_2, Fenton-like and photoFenton-like processes

Experimental conditions	k/kref
UV/H_2O_2	1
H_2O_2	0
$CuSO_4$	0
UV/$CuSO_4$	<0.07
H_2O_2/$CuSO_4$	<0.16
UV/H_2O_2/$CuSO_4$	2.02
UV/H_2O_2/$CuC1_2$	1.91
UV/H_2O_2/$KCr(SO_4)_2$	1.12

In order to elucidate the mechanism of the degradation, we attempted to identify the main intermediates. An incompletely photoreacted solution was also extracted with diethylether at pH >13 and evaporated under reduce pressure. The residue was dissolved in acetone-d_6 and analyzed by ^{1}H NMR. spectroscopy. Signals were observed at 7.35, 7.30, 6.90 and 2.80 ppm. They coincide with those of a pure sample of *N*,*N*-dimethylaniline. Formation of this amine was confirmed by GC/MS and HPLC analysis. Products **2**–**8** and **11**–**16** were identified too by means of GC/MS after derivatization. The identification was made by comparison with commercially available standards (compounds **2**, **3**, **4**, **8**, **11**–**14**, **16**) or with mass spectra reported in the literature (products **5**, **6**, **7**, **15**). Compounds **9** and **10** were isolated by thin layer chromatography using methylene chloride as the eluent (Table 3). Their structure was elucidated by ^{1}H NMR. spectroscopy (see Section 2).

Table 3
Organic compounds detected in the course of UV/H_2O_2 oxidation of the dye AO52 (except compound **18**, see text)

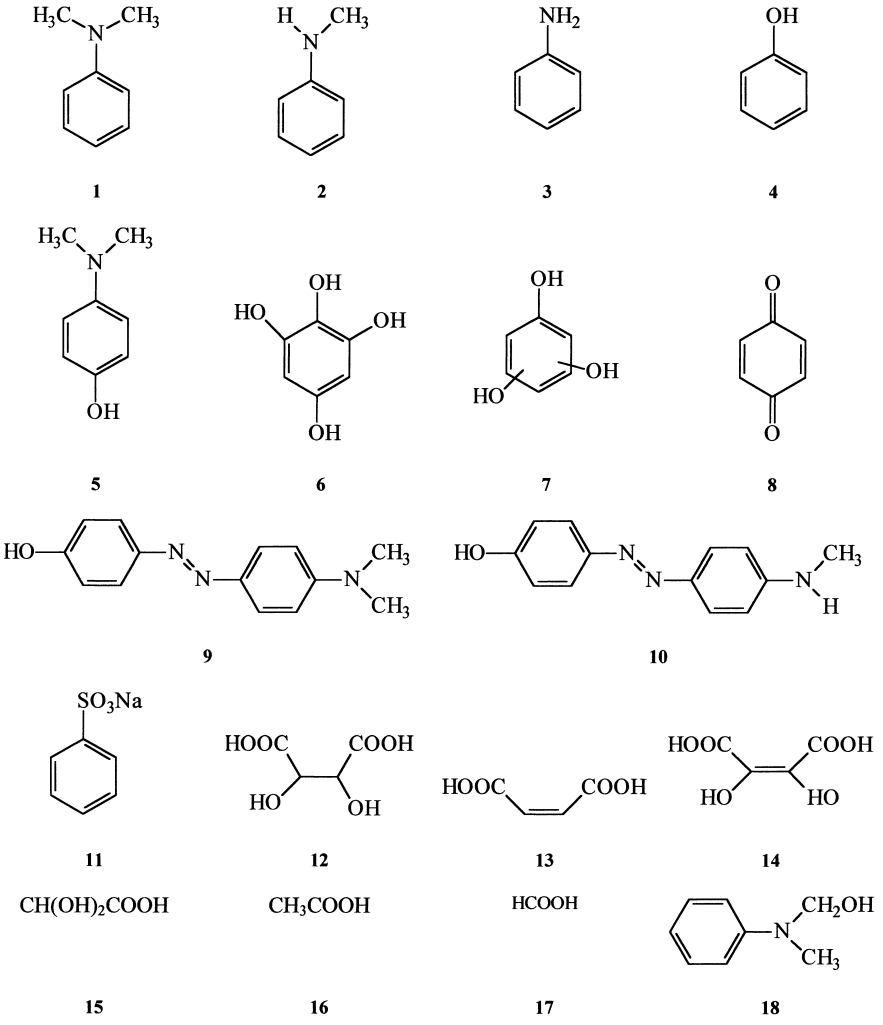

Some experiments were conducted in deuterium oxide and directly analyzed by NMR spectroscopy. This technique shows that a signal at 8.4 ppm appears since the first minutes of irradiation (Fig. 3b). It is ascribed to the very deshielded proton in formic acid (**17**). Assignment of this intermediate was confirmed by comparing ^1H shifts for spectra obtained during the photoreactions and for the pure acid. Formic acid is known as being the ultimate organic by-product of aromatic ring opening, but it may originate from the methyl groups of AO52.

Hydroxyl radicals, produced upon photolysis of hydrogen peroxide, are electrophilic oxidants. Consequently, oxidation of the dye must be initiated by the attack of $OH^{\bullet}$ upon an electron-rich site, i.e. on the amino group or near the azo nitrogen atoms. Detection of products **1**, **2**, **3**, **5**, **10** and **11** indicates that both decomposition pathways are involved. Loss of both N-methyl groups has already been reported on sensitized photooxidation [13–14]. In accordance with Darwent study [13], it is the first stage during the ZnO-assisted degradation of AO52. However its mechanism has not yet been completely clarified. The reaction can be initiated by one-electron extraction from the amino substituent by hydroxyl radical. The resulting radical cation undergoes an oxidation to give an iminium ion, from which the secondary amine can be formed by solvolysis; in accordance with Scheme 1. It is also expected that the eliminated methyl groups are converted to formaldehyde and consequently to formic acid.

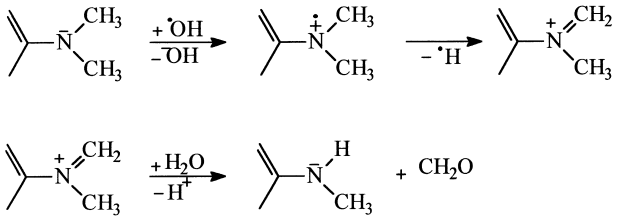

Scheme 1.

Another mechanism, which involves abstraction of a hydrogen atom by the hydroxyl radical was proposed. Aldehy-

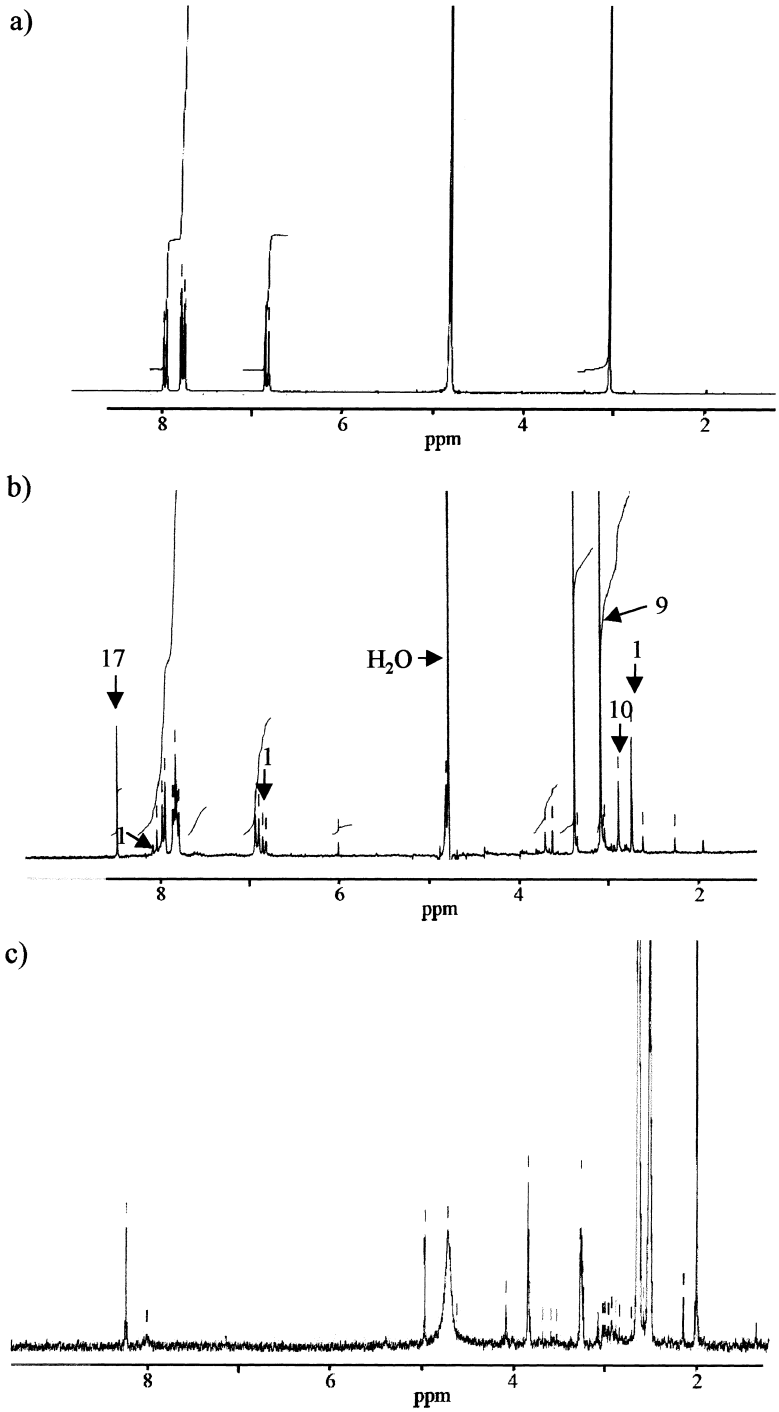

Fig. 3. ^{1}H NMR spectra of AO52 before the irradiation (a), at an intermediate time (AO52 degradation degree <50%) (b) and when the solution is completely discolored (c) (solvent: D_2O).

des and alcohols are postulated to be intermediary products [15–16]. They were not detected during AO52 degradation, but compound **18** was identified by GC/MS in the course of *N*,*N*-dimethylaniline decomposition. Consequently, we can assume that even if both mechanisms usually compete, the one-electron extraction from the amino substituent seems to be predominant during AO52 degradation. We can also note that the absorption maximum on the UV–VIS spectra exhibits a gradual hypsochromic shift in the course of illumination. This phenomenon can well be explained by *N*-demethylation.

On the other hand, based upon the observation of *N*,*N*-dimethylaniline, breaking of the original dye near its azo linkage may precede dealkylation. Spadaro et al. [17]

Table 4
Formulas of additional dyes

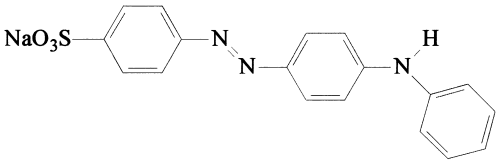

19

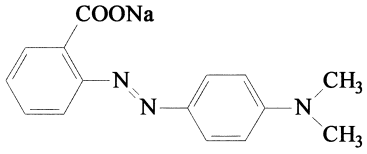

20

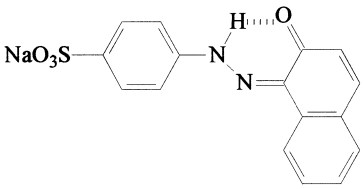

21

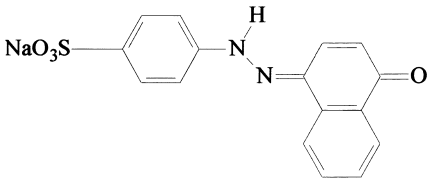

22

proposed that oxidation of aminoazobenzene dyes proceeds by the addition of an hydroxyl radical to the carbon atom bearing the azo bond, followed by the breaking of the resulting adduct. In our case, benzenesulfonic acid, *N,N*-dimethylaniline and 4-hydroxy-*N,N*-dimethylaniline may arise from such a series of reactions. However the powerful electronwithdrawing sulfonate group in AO52 molecules inhibits reactivity of the ring which carries it, as far as an electrophilic addition is concerned. Consequently the benzene ring, called '2' should be the first target of hydroxyl radicals. Our results show that it is not necessarily the case, presumably due to the very high reactivity of $OH^{\bullet}$ radicals toward organic compounds. This phenomenon also appears in the course of other dye degradation investigated in the laboratory, for instance AOS (**19**) and AR2 (**20**) with the production of respectively diphenylaniline and *N*-dimethylaniline (Table 4).

Whereas preceding mechanisms are in agreement with the electrophilic character of hydroxyl radicals, production of **9** and **10** is more surprising. Indeed, these by-products are the logic consequence of addition of $OH^{\bullet}$ on the carbon atom bearing the sulfonate group and the subsequent elimination of SO_3. Two parameters are against this reaction: the electronwithdrawing character of the sulfonate substituent and steric hindrance. However, a similar reaction was observed during the degradation of the aminoazobenzene AO5 and of the hydroxy azo dye AO7 (**21**) [18]. In the latter case, it was observed that the yield of the OH-adduct increases with the hydroxyl radical concentration in the solution. This reaction is also presumed not to be the major oxidation way.

The GC/MS procedure should have been able to detect muconic acid. The absence of this product and the formation of tri- and tetra-hydroxylated aromatic compounds suggests that aliphatic acids with two or four carbons are certainly formed via polyhydroxylation of benzene derivatives, followed by ring rupture.

An important point is that most of the identified aromatic by-products are very toxic. Some of them, for instance phenol, are subject to strict standards. It is therefore necessary to evaluate their lifetime in the solution. The complete bleaching is achieved after 350 min of irradiation and the absorbance in the 220–400 nm region is greatly reduced as well. Consequently, AO52 and most of by-products with an extended conjugated system, i.e. benzene derivatives, disappeared during the discolouration stage. That means that primary break-down products fortunately underwent further oxidation leading to aliphatic compounds and finally that they are at least as well sensitive to $OH^{\bullet}$-induced degradation as the original dye. Fig. 3 indicates that signals relative to high shield protons (1.9 ppm, between 3.3 and 4.5 ppm) in aliphatic species appear on the ^1H NMR spectrum of a incompletely photoreacted solution. They still exist when the solution is discoloured (spectrum 3c), but, as expected, no significative signal relative to aromatic products can be observed yet.

Moreover, in the course of the degradation, the inorganic anion SO_4^{2-} and carbon dioxide should be progressively formed. However, whereas the quantity of sulfate ions expected from a complete mineralization is obtained within 350 min, the profile of total organic carbon (TOC) versus time is sigmoidal with an inflection point, as illustrated in Fig. 4. It is worth noting that when the overall aromatic compounds are converted to aliphatic derivatives, i.e. at the end of the bleaching period, less than 30% of the stoichiometric amount of carbon dioxide is produced. Consequently the cleavage of benzene rings is only slightly implied in the carbon loss and the mineralization mainly refers to the destruction of aliphatic intermediates. Moreover, the inflection point is associated with a decrease in the photomineralization rate. This is an indication of the formation of some long-living aliphatic by-products. Indeed, even an extended irradiation, over 37 h, does not induce a complete conversion of the organic matter to water, carbon dioxide and in-

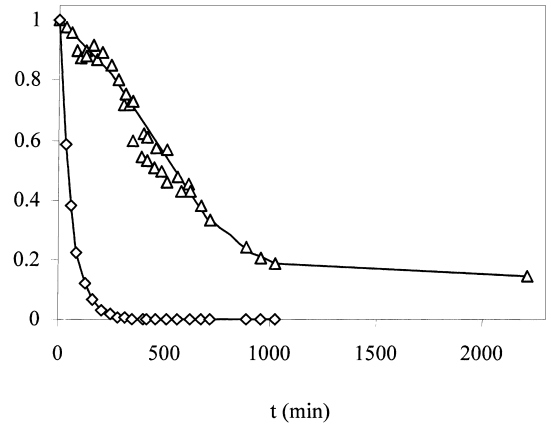

Fig. 4. Normalized total organic carbon (△) and colour removal (◇) during the UV/H_2O_2 oxidative treatment. $[AO52]_0 = 10^{-3}$ M-$[H_2O_2]_0 = 2 \times 10^{-1}$ M; initial pH = 5.5 – rT.

organic species. This result totally agrees with the low rate constants of reactions between hydroxyl radicals and some aliphatic acids [19].

3.2. Oxidation of the dye AO52 by the UV/TiO_2 advanced oxidation process

The use of semiconductors, for instance TiO_2, as photocatalysts has been extensively studied [20]. It has the large advantage over the UV/H_2O_2 method not to require an irradiation by costly far UV, because titanium dioxide absorbs light up to 385 nm. We realize that solutions of AO52 at concentrations commonly found in textile effluents (10^{-4}–10^{-6} M) can be completely discoloured using a black-light mercury lamp as a UV radiation source.

Literature [21,22] indicates that the first step of the photocatalytic degradation of aromatic compounds often corresponds to the formation of hydroxylated derivatives. The product distribution may be modified when a hydroxyl radical scavenger is added to the solution [23]. This suggest that two types of oxidizing species are involved in the photocatalytic process: hydroxyl radicals, generated by oxidation of adsorbed water molecules (Eq. (12)) and positive holes. The efficiency of the degradation depends on the oxygen concentration since O_2 scavenges the conduction band electron, preventing (e^-, h^+) recombination. The overall process can be depicted by Eqs. (11)–(16).

$$TiO_2 + h\nu(UV) \rightarrow TiO_2(e^-, h^+) \quad (11)$$

$$TiO_2(h^+) + H_2O_{ads} \rightarrow TiO_2 + H^+ + OH_{ads}^{\bullet} \quad (12)$$

$$TiO_2(h^+) + HO_{ads}^- \rightarrow TiO_2 + OH_{ads}^{\bullet} \quad (13)$$

$$O_2 + TiO_2(e^-) \rightarrow TiO_2 + O_2^{\bullet -} \quad (14)$$

$$OH_{ads}^{\bullet} + \text{dye} \rightarrow \text{degradation of the dye} \quad (15)$$

$$h^+ + \text{dye} \rightarrow \text{dye}^{\bullet +} \rightarrow \text{oxidation of the dye} \quad (16)$$

On the kinetic viewpoint, the solute shows a fairly good linear relation between [solute] and irradiation time. This behaviour can be rationalized in terms of modified forms of the Langmuir–Hinshelwood kinetic treatment, which have already been successfully used to describe solid–liquid reactions [24]. The rate of unimolecular surface reaction is proportional to the surface coverage, assuming that the reactant is more strongly adsorbed on TiO_2 particules than the products:

$$r_{LH} = -\frac{dC}{dt} = \frac{kKC}{1 + KC} \quad (17)$$

with C is the concentration of the dye at time t; k the second order rate constant ($M^{-1}\,s^{-1}$); K the adsorption constant ($l\,mol^{-1}$).

The integrated form of Eq. (17) is

$$t = \frac{1}{Kk}\ln\frac{C_0}{C} + \frac{1}{k}(C_0 - C) \quad (18)$$

Since the contaminant is dilute, the second terms of the expression becomes small compared with the first one and under these conditions:

$$\ln\frac{C_0}{C} \approx kKt = k't \quad (19)$$

On the other hand, it must be borne in mind that the zero point of charge of Degussa P25 TiO_2 in aqueous solution is 6.8. The variations in the initial pH cause changes in the amount of AO52 adsorbed upon equilibration in the dark. At pH < 6, the positively charged titanium dioxide offers a suitable surface for non-protonated AO52 molecule adsorption. The extend of adsorption of AO52 on titanium dioxide at pH = 4.7 was also measured monitoring the solute concentration in the bulk solution before and after the adsorption–desorption equilibrium was reached. The behaviour of the number of dye adsorbed moles per gram of TiO_2, called n, as a function of the equilibrium concentration, C_{eq}, can be expressed as followed:

$$n = \frac{n_{max}KC_{eq}}{1 + KC_{eq}} \quad (20)$$

where n_{max} is the total number of adsorption sites and K is the above-mentioned adsorption constant, which reflects the proportion of solute molecules anchored to the surface. Eq. (21) is more instructive. Indeed, plot of C_{eq}/n versus C_{eq} gives a value of $15.5 \times 10^3\,l\,mol^{-1}$ for the coefficient K and $1.5 \times 10^{-5}\,mol\,g^{-1}$ for n_{max} at natural pH. As the total number of adsorption sites available is about $4 \times 10^{-4}\,mol\,g^{-1}$ [25], we can deduce that adsorbed dye molecules are surrounded by many anchored water molecules, which are involved in the degradation process.

$$\frac{C_{eq}}{n} = \frac{1}{Kn_{max}} + \frac{C_{eq}}{n_{max}} \quad (21)$$

Comparison of KBr/AO52 and TiO_2/AO52 FTIR spectra, in the 1900–1000 cm^{-1} region (Fig. 5), affords us to gain in-

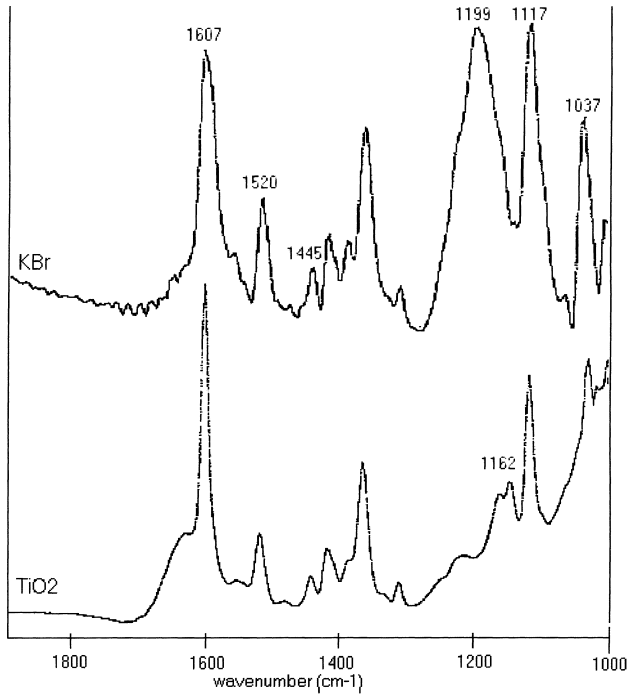

Fig. 5. Comparative infrared spectra of AO52 adsorbed on KBr and on TiO_2.

formations on the character of the TiO_2/dye interaction, i.e. chemisorption or physisorption. A similar study has being carried out with the 4-(2-hydroxy-1-naphthylazo)benzenesulfonic acid sodium salt, commonly named acid orange 7 (AO7) in our laboratory [26]. Authors suggest that adsorption of the dye on the surface of the semiconductor involves oxygen atoms of the sulfonate group, with the formation of a bidentate structure. They based their argument on the relative decrease and significant shifts in the peaks ascribed to the substituent. Indeed, in our case, such a phenomenon is observed: the peak at 1199 cm^{-1}, due to an asymmetric stretching vibration in the $–SO_3Na$ group [27], is shifted to 1162 cm^{-1} after adsorption on TiO_2, and its intensity decreases sharply. The other bands relative to symmetric (1037, 1117 cm^{-1}) and asymmetric (1223 cm^{-1}) vibrations of the electronwithdrawing substituent are shifted to a smaller extent to lower wavenumbers. Consequently, there are actually changes in these internal molecular bond energies. Moreover, KBr/AO52 spectrum exhibits C=C aromatic ring stretching vibrations peaks at 1607, 1520 and 1445 cm^{-1}. The growth in the height of the 1607 cm^{-1} band after adsorption indicates that the aromatic part of the molecule loses some degrees of freedom. Hence, as the molecule is strongly anchored on the TiO_2 surface, the nitrogen atom of the amino group, which is a relatively strong electron donor, may efficiently interact with trapped holes. It is worth noting that the weak intensity of the –N=N– band, and the fact that it probably arises in the 1450–1600 cm^{-1} region along with aromatic absorptions, therefore appear to preclude any useful correlation with this group.

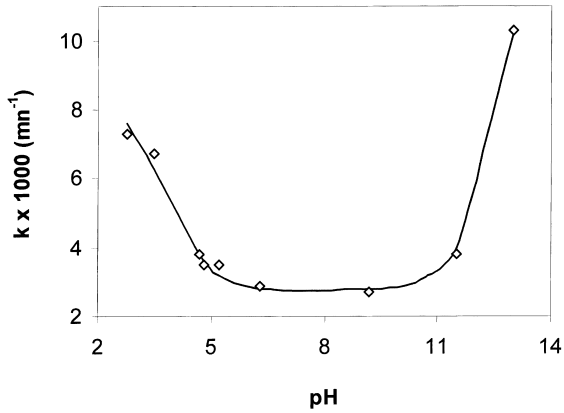

Fig. 6. Influence of the pH on the efficiency of the UV/TiO_2 process. $[AO52]_0 = 5 \times 10^{-5}$ M; TiO_2: 5×10^{-1} g l^{-1} – rT.

As dye molecules are negatively charged in alkaline media, their adsorption is also expected to be affected by an increase in the density of TiO^- groups on the semiconductor surface. Due to the Coulombic repulsion, no direct electrostatic interaction between AO52 and TiO_2 particules can occur.

As a consequence, the coverage of the oxide surface is distinctly pH-dependent. There is every indication that the pH of the solution may also influence the reaction rate. Indeed, as illustrated in Fig. 6, whereas *k* remains constant in the pH range 5–10, it dramatically increases at extreme pH values. This might suggest that different mechanisms take place. We can venture the hypothesis that at pH > 7, as previously mentioned, the large distance between the reagents does not allow a direct charge transfer and the decomposition of AO52 molecules mainly depends on diffusion of surface-generated hydroxyl radicals to the anion in the double layer. With the purpose to check this hypothesis, the effect of chemical competition on the photodegradation of AO52 was investigated. Increasing quantities of methanol or sodium benzoate — two efficient hydroxyl radical scavengers — were added to the suspension at initial pH = 9.2. In both cases, the degradation of the dye is partly quenched, and the reciprocal of the reaction rate increases linearly with the scavenger concentration [S], due to a competition between AO52 and the scavenger with respect to the photogenerated oxidant X, according to Scheme 2.

The slope of $1/r_1 = f([S])$ gives the relative rate for both scavengers with the oxidative agent. The ratio we obtain is close to the value reported in the literature assuming that free $HO^\bullet$ is the only oxidizing species. This result completely agrees with our hypothesis. Moreover, in very alkaline solutions (pH > 10), since hydroxyl radicals are easier to be generated by oxidizing more hydroxide ions available on TiO_2 surface, the efficiency of the process is logically enhanced (Table 5).

The increase of the proportion of solute molecules anchored to the oxide surface in slightly acid suspensions might also explain the rise in the degradation rate at pH values

TiO_2 + hν	→	X	$r_{(X)}$
X + AO52	→	oxidation of the dye	$r_1 = k_1$ [AO52] [X]
X + Scavenger	→	degradation of the scavenger	k_2 [S] [X]
X + M	→	reaction with M	k_3 [M] [X]

with M: impurities or photoproducts

Scheme 2.

Table 5
Comparison between rate constants determined with illuminated aqueous slurries of TiO_2 and mean published HO rate constants

Scavenger	Relative rate for the UV/TiO_2 system ($pH_0 = 9.2$)	Relative rate for S + HO•
Methanol	1.0	1.0
Sodium benzoate	5.0	5.2

up to 4.7. However, an other factor must be involved to account for the further drastic increase in the discolouration rate at lower pH. Indeed, in aqueous solution, AO52 is an anion, whose absorption spectrum remains invariant in the pH range 4–14, but changes below pH ≈ 4, as expected for protonation of the β nitrogen atom of the azo linkage [28]. Whereas the unprotonated compounds is an electron donor, the zwitterion has a marked electronwithdrawing character. We can assume then that the conduction band electron in TiO_2 particules may be directly picked up by protonated dye molecules, leading to the production of the dye anion radical. The latter can undergo subsequent reactions leading to the degradation of the coloured compound. However whereas this electron transfer can readily compete with electron trap by O_2, it is less efficient than the inhibition of the electron–hole recombination by hydrogen peroxide. Indeed experiments conducted in the presence of this additive show a sharp increase (by more of 30) the discolouration rate. This phenomenon can be explained by the formation of hydroxyl radicals according to Eq. (22), and by their subsequent reaction with protonated dye molecules, since the latter are very susceptible to HO•-induced oxidation [12].

$$TiO_2(e^-) + H_2O_2 \rightarrow TiO_2 + OH^- + OH^\bullet \quad (22)$$

FTIR was also used to follow the progress of the reaction on a thin layer of titanium dioxide (about 150 μm thick) coated with AO52. The spectra recorded after various times following UV irradiation are shown in Fig. 7.

Changes in the spectra indicate that degradation of adsorbed AO52 molecules has occurred. The IR was operated in transmission mode. This mode was selected to take advantage of the linear absorbance signal dictated by Beer's law and due to the inherent difficulties involved in quantitative reflectance methods. At the beginning of the irradiation, decomposition of the original dye is linked to the decrease of the intensity of the bands at 1607 and 1368 cm^{-1}. Indeed, these peaks respectively reflect the destruction of

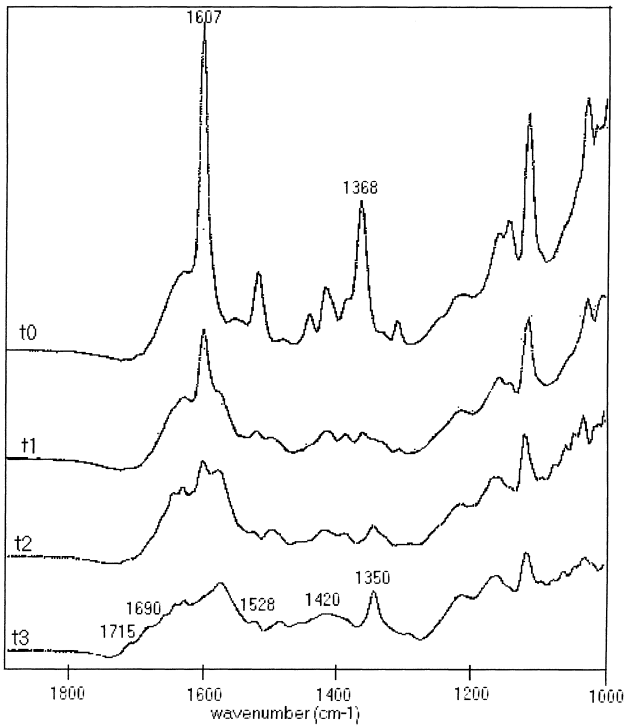

Fig. 7. UV/TiO_2 process: Infrared spectra of AO52 adsorbed on fresh TiO_2 and after increasing irradiation times (193, 447, 1409 mn).

the aromatic part of the molecule and the elimination of the amino group. Thereafter, this correlation is no longer observed, due to the appearance of new bands associated to breakdown products in these regions. Increasing number of compounds absorbing at 1350 cm^{-1} is observed. At first sight, it can be ascribed to nitrate ions, to a symmetric stretching in aryl nitro products or to a –C–N– stretching vibration in a N-substituted derivative of AO52 (for instance *N*,*N*-dimethylaniline). However, the latter possibilities can be excluded. Indeed, on one hand, none of the other characteristic bands of substituted anilines are detected on the different spectra. On the other hand, the simultaneous appearance of an aromatic skeletal vibration band at 1528 cm^{-1} may suggest the formation of nitrobenzene [29]. Nevertheless, the intensities of the peaks located at 1528 and 1350 cm^{-1} do not evolve similarly, as illustrated in Fig. 8. Whereas the former stabilises after approximately 450 min, the band at 1350 cm^{-1} still increases according to first order kinetics. It is reasonable to conclude therefore that they do

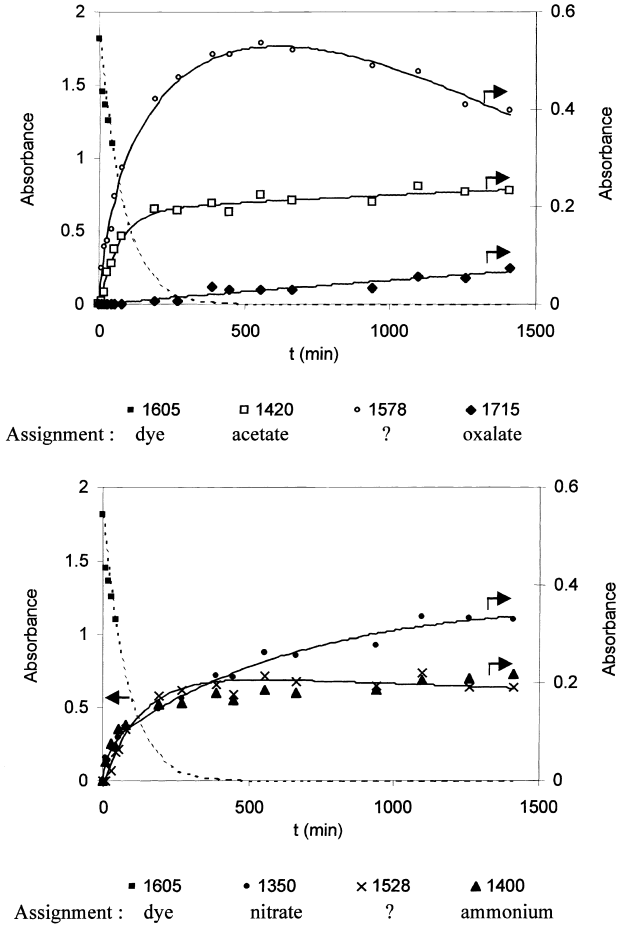

Fig. 8. Evolution of the absorbance at characteristic wavenumbers during the UV/TiO_2-induced oxidation of AO52.

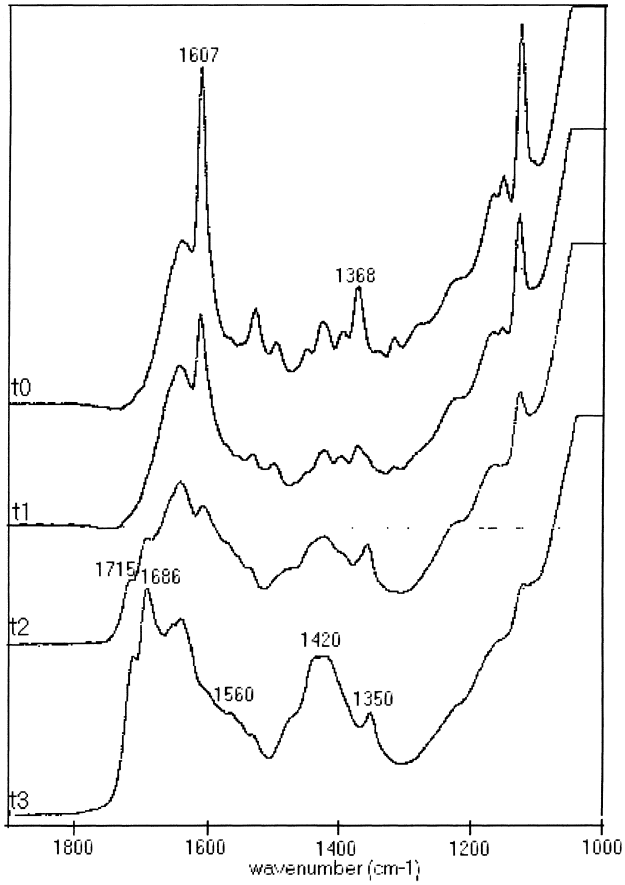

Fig. 9. VIS/TiO_2 process Infrared spectra of AO52 adsorbed on fresh TiO_2 and after increasing irradiation times (28, 128, 586 nm).

not refer to the same intermediate. In fact, under UV/TiO_2 assisted oxidation, one can expect that nitrogen contained in AO52 molecules can be transformed into nitrate ions, and also into gaseous N_2, nitrite and ammonium ions. Since no new band is found between 1230 and 1250 cm^{-1}, we can deduce that either inorganic nitrites are not produced during the process or they are not stable enough to be detected. On the contrary, traces of bands associated to the ammonium cation can be observed on our samples, according to shoulders at 1400 and 1455 cm^{-1} [30–31].

Moreover, after a few minutes, two bands appear at 1715 and 1690 cm^{-1} (Fig. 7). Their positions are identical to those of carbonyl vibrations in the spectrum of sodium oxalate adsorbed on TiO_2. This aliphatic species accumulates during the process. Likewise, the intensity of the band at 1420 cm^{-1}, ascribed to an interaction between the C–O stretching and the O–H bending of carboxylic acid [32], probably acetic acid, increases gradually. Moreover many bands occur at 1570–1665 cm^{-1}, i.e. in the region ascribed to free-ionized COO stretching. We can mention that the intensities of the peaks at 1528, 1578, 1632, 1647 and 1663 cm^{-1} evolve similarly, i.e. the absorbance reaches a maximum level after about 450 min of irradiation. Finally only aliphatic and inorganic species can be detected during AO52 degradation. That means that aromatic derivatives are very susceptible to oxidation.

Note that irradiation is necessary for the oxidation to occur since control experiments have shown that no thermal reaction takes place when an incompletely degraded wafer is maintained a few hours in the dark after irradiation.

3.3. Oxidation of the dye AO52 by the VIS/TiO_2 advanced oxidation process

Such experiments were conducted using a He–Cd laser, generating a 442 nm monochromatic light, which prevents direct absorption of light by the semiconductor (TiO_2 only absorbs light up to 385 nm). Substantial changes were observed by FTIR spectroscopy upon photolysis of AO52/TiO_2 sample, suggesting that the dye undergoes degradation (Fig. 9), i.e. excited AO52 is able to inject an electron into the conduction band of the semiconductor. Usually, the VIS/TiO_2 photocatalysis of a dye D involves following reactions:

$$D + h\nu(\text{visible}) \rightarrow D^* \quad (23)$$

$$D^* + TiO_2 \rightarrow D^{\bullet +} + TiO_2(e^-) \quad (24)$$

$$TiO_2(e^-) + O_2 \rightarrow TiO_2 + O_2^- \quad (25)$$

$$D^{\bullet+} \rightarrow \text{degradation of } D^{\bullet+} \quad (26)$$

The dye molecule that has lost an electron (i.e. $D^{\bullet+}$) readily reacts with hydroxyl ions undergoing oxidation via steps 27 and 28 or interacts effectively with $O_2^{\bullet-}$, $HOO^{\bullet}$ or $HO^{\bullet}$ species to generate intermediates that ultimately lead to CO_2 (Eq. (29)–(33))

$$D^{\bullet+} + HO^- \rightarrow D + HO^{\bullet} \quad (27)$$

$$D + 2HO^{\bullet} \rightarrow H_2O + \text{oxidation products} \quad (28)$$

$$O_2^{\bullet-} + H^+ \rightarrow HOO^{\bullet} \quad (29)$$

$$HOO^{\bullet} + H^+ + TiO_2(e^-) \rightarrow H_2O_2 + TiO_2 \quad (30)$$

$$H_2O_2 + TiO_2(e^-) \rightarrow HO^{\bullet} + HO^- + TiO_2 \quad (31)$$

$$D^{\bullet+} + O_2^{\bullet-} \rightarrow DO_2 \rightarrow \text{products} \quad (32)$$

$$D^{\bullet+} + HOO^{\bullet}(\text{or } HO^{\bullet}) \rightarrow \text{products} \quad (33)$$

Irradiation of an aqueous suspension of TiO_2 indicates that AO52 decomposition is relatively slow compared to phenylazonaphthols. Indeed, complete bleaching requires nearly 100 h, whereas, under the same experimental conditions (3 ml, $[dye]_0 = 5 \times 10^{-5}$ M, TiO_2 loading: 1 g l^{-1}), only 2 h are needed for the hydroxy monoazo dye AO20 (**22**). It must be emphasized that at low concentrations of dye AO52, the discolouration of the solutions is governed by first-order kinetics, as for preceding AOPs. However, in the present case, the irradiation times are too long to permit further kinetic investigations.

Analysis of the FTIR spectra provides some insight into the nature of the photoproducts (Fig. 9). Many signals obtained during the photocatalytic process can also be detected: sodium acetate (1420 cm^{-1}), sodium oxalate (1686 and 1715 cm^{-1}) and inorganic nitrates (1350 cm^{-1}) are undisputably produced. Intensities of the corresponding bands are higher than during the UV/TiO_2 oxidation, especially for oxalates, as illustrated on Fig. 10. In fact, these adsorbed breakdown products do not absorb at 442 nm, so that they cannot be involved in the photosensitizing process and consequently they accumulate. We must also notice the absence of the band located at 1578 cm^{-1} and the appearance of a peak at 1563 cm^{-1}, that some authors assigned to formate ions [33]. Finally, an important point is that whatever the irradiation wavelength is (UV or visible light), only aliphatic substracts are detected at the end of the process. But, all the same, in heterogeneous solution, the combined action of visible light and TiO_2 does not seem to be an efficient method to induce the degradation of the aminoazobenzene AO52, although the quantum yield of the oxidation was not determined in this study.

4. Conclusion

The results of our study have shown that both UV/H_2O_2 and UV/TiO_2 can be efficiently used to degrade the aminoazobenzene AO52. Although the VIS/TiO_2 seems to be less effective on the kinetic viewpoint, the capability of the excited aminoazobenzene to inject an electron in the conduction band of the semiconductor could be turn to good account combining UV and visible irradiations, i.e. using non-expensive sunlight as radiation source.

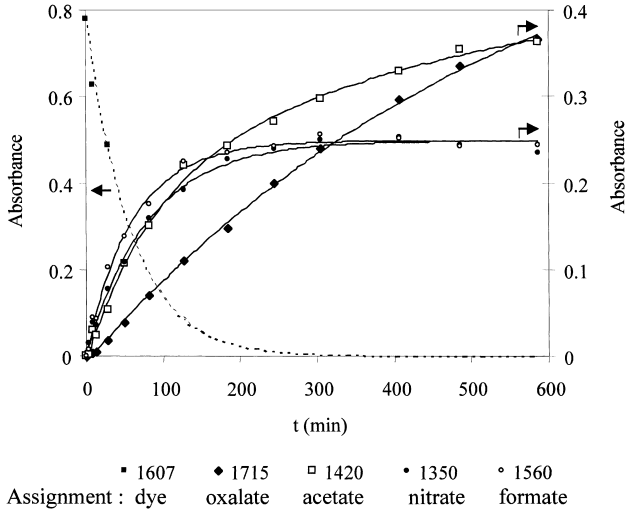

Fig. 10. Evolution of the absorbance at characteristic wavenumbers during the VIS/TiO_2-induced oxidation of AO52.

An important point is that many aromatic toxic breakdown products, especially aniline derivatives, are detected during the bleaching stage for the UV/H_2O_2 process, but not for both heterogeneous systems. This report suggests that in the TiO_2-assisted photodegradations, the intermediates generated in the initial stages absorb on the oxide surface and undergo further fast decomposition until they are completely transformed into CO_2 or into aliphatic acids, which react rather slowly with hydroxyl radicals or trapped holes. The latters can also be easily detected by FTIR spectroscopy. However it is to be feared that these acids, due to their weak susceptibility to oxidation, become poisons for the oxide by blocking active sites. Thus any impulse to extend these results to an economical application should be preceded by an evaluation of the turnover of the semiconductor.

Acknowledgements

The authors thank Pr. B. Muckenstürm and his staff of the Laboratoire de Chimie des plantes of ENSCMu for the GC/MS analysis and Dr Le Nouen, of the Laboratoire de Chimie et Pharmacologie Organiques for the ^{1}H NMR and NMR-C13 analysis.

References

[1] P. Aires, F. Gal, E. Chamarro, S. Esplugas, J. Photochem. Photobiol. A. Chem 68 (1992) 121–129.
[2] W.H. Glaze, J.W. Kang, Ind. Eng. Chem. Res. 28 (1989) 1573–1580.

[3] N. Karpel Vel Leitner, R. Ben Abdessalem, M. Doré, New. J. Chem. 21 (1997) 187–194.
[4] K.H. Gregor, Melland Textilber. 71 (1990) E435–E436, 976–979.
[5] H.-Y. Shu, C-R. Huang, Chemosphere 31 (1995) 3813–3825.
[6] D. Nansheng, T. Shizhong, X. Mei, Water. Qual. Res. J. Can. 30 (1995) 53–59.
[7] N.H. Ince, D.T. Gönenç, Environ.Technol. 18 (1997) 179–185.
[8] H. Christensen, K. Sehested, H. Corfitzen, J. Am. Chem. Soc 86 (1982) 1588–1590.
[9] R.W. Matthews, H.A. Mahiman, T.J. Sworski, J. Phys. Chem. 76 (1972) 1265–1272.
[10] P. Neta, V. Madhavan, H. Zemel, R.W. Fessenden, J. Am. Chem. Soc. 99 (1977) 163–164.
[11] J.L. Weeks, J. Rabani, J. Phys. Chem 70 (1966) 2100–2106.
[12] C. Galindo, A. Kalt, Dyes Pigments 42 (1998) 27–35.
[13] J.R. Darwent, A. Lepre, J. Chem. Soc. Faraday Trans. 2 82 (1986) 1457–1468.
[14] T. Watanabe, T. Takizawa, K. Honda, J. Phys. Chem. 81 (1977) 1845.
[15] J.C. Milano, P. Loste-Berdot, J.L. Vernet, Env. Technol. 16 (1995) 329–341.
[16] D.G. Crosby, C.S. Tang, J. Agric. Food. Chem. 17 (1969) 1041–1044.
[17] J.T. Spadaro, I. Lorne, V. Renganathan, Environ. Sci. Technol. 28 (1994) 1389–1393.
[18] C. Galindo, P. Jacques, A. Kalt, J. Adv. Oxid. Technol. in press.
[19] N. Karpel Vel Leitner, M. Doré, J. Photochem. Photobiol. A: Chem. 99 (1996) 137–143.
[20] O. Legrini, E. Oliveros, A.M. Braun, Chem. Rev. 93 (1993) 671–698.
[21] G. Al-Sayyed, J.-C. D'Oliveira, P. Pichat, J. Photochem. Photobiol. A: Chem. (1991) 99–114.
[22] R.W. Matthews, J. Chem. Soc. Faraday Trans. 1 80 (1984) 457–471.
[23] S. Golstein, G. Czapski, J. Rabani, J. Phys. Chem. 98 (1994) 6586–9591.
[24] R.W. Matthews, J. Phys. Chem. 91 (1987) 3328–3333.
[25] J. Cunningham, G. Al-Sayyed, S. Srijaranai, Aquatic and Surface Chemistry, G.R. Helt, R.G. Zepp, D.G. Crosby (Eds.), Lewis Publishers, Boca Raton, FL, 1994, p. 317.
[26] C. Bauer, P. Jacques, A. Kalt, Chem. Phys. Lett. 307 (1999) 397–406.
[27] R.N. Haszeldine, J.M. Kidd, J. Chem. Soc. (1954) 4228–4233.
[28] K.M. Tawarah, H.M. Abu-Shamleh, Dyes Pigments 16 (1991) 241–251.
[29] D.H. Williams, I. Fleming, Spectroscopic Methods in Organic Chemistry, 4th ed., McGraw-Hill Book Company, 1989, p. 54.
[30] M. Hermann, H.P. Boehm, Z Anorg. Allg. Chem. 368 (1969) 73.
[31] R. Mendez-Roman, N. Cardona-Martinez, Catal. Today 40 (1998) 353–365.
[32] J.M. Gallardo Amores, V. Sanchez Escribano, R. Gianguido, G. Busca, Appl. Catal. B: Environ. 13 (1997) 45–58.
[33] G. Busca, J. Lamotte, J.-C. Lavalley, V. Lorenzelli, J. Am. Chem. Soc. 109 (1987) 5197–5202.